Anal Bioanal Chem (2005) 383: 532–538
DOI 10.1007/s00216-005-0034-5

ORIGINAL PAPER

Shyh-Hwang Lee · Hung-Yuan Fang · Wen-Chang Chen · Hong-Ming Lin · C. Allen Chang

Electrochemical study on screen-printed carbon electrodes with modification by iron nanoparticles in $Fe(CN)_6^{4-/3-}$ redox system

Received: 25 April 2005 / Revised: 13 July 2005 / Accepted: 14 July 2005 / Published online: 1 September 2005

Abstract The remarkable enhancement of electron transfer on screen-printed carbon electrodes (SPCEs) with modification by iron nanoparticles (Fe_{nano}), coupled with $Fe(CN)_6^{4-/3-}$ redox species, was characterized with an increase of electroactive area (A_{ea}) at electrode surface together with a decrease of heterogeneous electron transfer rate constant ($k°$) in the system. Hence, Fe_{nano}-$Fe(CN)_6^{3-}$ SPCEs with deposition of glucose oxidase (GOD) demonstrated a higher sensitivity to various glucose concentrations than $Fe(CN)_6^{3-}$/GOD-deposited SPCEs. In addition, an inhibited diffusion current from cyclic voltammograms was also observed with an increase in redox concentration and complicated the estimation of A_{ea}. Further analysis by the electrochemical impedance method, it was shown that this effect might be resulted from the electrode surface blocking by the products of activated complex decomposition.

Keywords Heterogeneous electron transfer rate constant · Electroactive area · Screen-printed carbon electrode · Iron nanoparticles · $Fe(CN)_6^{4-/3-}$ redox couple

S.-H. Lee
Graduate School of Engineering Science and Technology,
National Yunlin University of Science & Technology,
123 University Road, Sec. 3, Douliou,
Yunlin, Taiwan, ROC

H.-Y. Fang
Department of Safety,
Health and Environmental Engineering,
National Yunlin University of Science & Technology,
123 University Road, Sec. 3, Douliou,
Yunlin, Taiwan, ROC

W.-C. Chen (✉)
Department of Chemical Engineering,
National Yunlin University of Science & Technology,
123 University Rd., Sec. 3, Douliou,
Yunlin, 640, Taiwan, ROC
e-mail: chenwc@yuntech.edu.tw
Tel.: +886-05-5342601

H.-M. Lin
Department of Materials Engineering,
Tatung University,
Taipei, Taiwan, ROC

C. A. Chang
Department of Biological Science and Technology,
National Chiao Tung University,
Hsinchu, Taiwan, ROC

Introduction

Over the past few years, screen printing seems to be one of the most promising technologies in the application of simple, rapid, inexpensive, and disposable biosensors in clinical and industrial analysis because of the advantages such as versatility, low cost, and particularly the possibility of mass production. In particular, amperometric biosensors fabricated via screen-printed carbon electrodes (SPCEs) have not only gained the interests of many research laboratories [1–5] but have also been commercially exploited in the fabrication of personal glucose biosensors for diabetics [6, 7].

Artificial redox mediators are often used to shuttle electrons between the embedded redox center of enzyme and the electrode surface for the amperometric biosensors [8, 9]. The ferro/ferricyanide [$Fe(CN)_6^{4-/3-}$] redox system used in this study exhibits a heterogeneous one-electron transfer and is one of the most extensively studied redox couples in electrochemistry [10, 11]. The scheme of the glucose biosensing mechanism with this redox species is shown in Fig. 1.

Many attempts have been made to modify SPCEs in the application of biosensors for enhancing the electron flow to some extent [12–14]. Iron nanoparticles (Fe_{nano}) is one of the popular nanomaterials [15] that are gaining interests to offer excellent prospects for chemical and biological sensing. In our laboratory, the preliminary experimental results showed that a simple way of Fe_{nano} modification on the surface of SPCEs could amplify the amperometric current with $Fe(CN)_6^{4-/3-}$ redox couples, hence increase the sensor sensitivity.

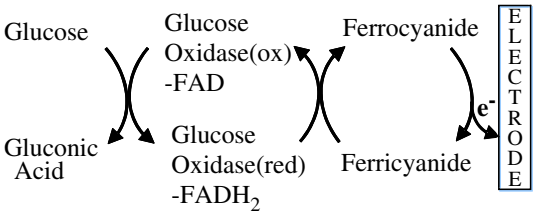

Fig. 1 The sequence of electron transfer in the ferricyanide-mediated glucose biosensor

Electroactive area (A_{ea}) related to redox probe system has been used to characterize the current amplification of modified electrodes using a fixed $Fe(CN)_6^{3-}$ concentration based on the assumption that the peak current was linearly proportional to the redox concentration [16–18]. However, the estimation of A_{ea} is complicated by the nonlinear responses of the cathodic peak current to the $Fe(CN)_6^{3-}$ concentration at the disposable SPCEs used in this work.

Previous reports [19–24] showed that the electron transfer process in the $Fe(CN)_6^{4-/3-}$ system was considerably more complex and could not be treated as a simple outer-sphere electron exchange between two species present in the solution. The effect of the supporting electrolyte cation on the electron transfer kinetics in $Fe(CN)_6^{4-/3-}$ redox system was postulated to be associated with ion-pair formation in the active complex containing the oxidized and reduced redox system species linked by the supporting electrolyte ions [19, 20]. Some authors suggested that platinum electrode surface was adsorbed by $Fe(CN)_6^{4-/3-}$ ion [21, 22] and partially blocked by the decomposition products of active complex [23, 24].

The main purpose of this study was to investigate the kinetics of the enhanced electron transfer in $Fe(CN)_6^{4-/3-}$ redox system on SPCEs with modification by Fe_{nano} and the inhibited diffusion current with an increase in redox concentration using cyclic voltammetry (CV) and electrochemical impedance spectroscopy (EIS). In addition, a higher sensitivity to varying glucose concentrations by Fe_{nano}-$Fe(CN)_6^{3-}$ SPCEs with deposition of glucose oxidase (GOD) was also presented.

Experimental

$K_3Fe(CN)_6$ and $K_4Fe(CN)_6$ were purchased from Merck, iron nanoparticles (Fe_{nano}) (25~100 nm) from Vacuum Metallurgical Co., Ltd. (Chiba, Japan), GOD (EC 1.1.3.4, 5,100 U mg protein^{-1}, from *Aspergillus niger*) and β-D-glucose were from Sigma (St. Louis, MO, USA). All other chemicals were analytical grade. Phosphate buffer solutions (PBS, 0.1 M) were prepared by mixing stock solutions of K_2HPO_4 and NaH_2PO_4, and pH values were adjusted with 0.1 M H_3PO_4 or NaOH solution. GOD solution was freshly prepared daily just before the fabrication of biosensors with PBS (pH 7.0) to give 0.6 U μl^{-1}. Glucose standard solutions (0–600 mg dl^{-1}) were prepared in PBS (pH 7.0), left overnight to allow equilibration of the anomers and stored at 4°C. Solutions of Fe_{nano} and Fe_{nano}-$Fe(CN)_6^{3-}$ were prepared by dissolving appropriate amounts of Fe_{nano} in PBS (pH 7.0) and in 0.1 M $Fe(CN)_6^{3-}$ solution, respectively. Double-distilled water (Millipore-Q) was used in this study. Disposable SPCEs test strips (gifts from Apex Biotechnology Corp., Hsinchu, Taiwan) with a two-electrode configuration were used for glucose biosensor fabrication. Each SPCEs test strip consists of two identical half-circular electrodes (with a diameter of 5 mm and a gap of 0.5 mm) that were used as the working and counter electrodes on a polyvinyl chloride substrate.

Electrochemical experiments including CV and chronoamperometry (CA) were performed using a CHI 440 electrochemical workstation (CH Instruments, USA). The EIS analyses were performed with an Autolab PGSTAT12 (Eco chemie, B.V., The Netherlands) and controlled by GPES 4.9 and FRA 4.9 softwares, and the impedance spectra were recorded in the frequency range of 0.1 Hz–100 kHz by using a sinusoidal excitation signal (single sine) with an excitation amplitude of 10 mV. All electrochemical measurements were determined at room temperature (25±1°C), and results were reported by taking the mean of the measurements in triplicate.

For kinetics study, Fe_{nano}-modified SPCEs were prepared by pipetting 10 μl Fe_{nano} solution onto the bare electrode surface and dried at 40°C for 15 min. CV and EIS measurements were conducted immediately after 10 μl redox solution was dropped on the bare or Fe_{nano}-modified SPCEs.

The fabrication of $Fe(CN)_6^{3-}$/GOD or Fe_{nano}-$Fe(CN)_6^{3-}$/GOD SPCEs was firstly deposited with 10 μl $Fe(CN)_6^{3-}$ or Fe_{nano}-$Fe(CN)_6^{3-}$ solution on the surface of bare SPCEs and dried at 40°C for 15 min. And then 5 μl GOD solution was layered-on and dried to be ready for use. For glucose sensing, the amperometric current-time response at a fixed potential of 0.3 V, following the addition of glucose solutions onto the biosensor test-strips, was recorded for 10 s, and the calibration plots of the glucose biosensors were constructed.

Results and discussion

Characterization of Fe_{nano}-modified SPCEs

CVs were conducted with Fe_{nano}-modified SPCEs in the presence of 0.1 M $Fe(CN)_6^{3-}$ over the potential range from −0.5 to +0.5 V at a scan rate of 0.05 V s^{-1}. A current amplification is observed with increase in Fe_{nano} loading on the modified SPCEs toward $Fe(CN)_6^{3-}$ redox reaction (Fig. 2). It implies that Fe_{nano} could act as a promising electroactive material for glucose biosensor.

In Fig. 2, the Fe_{nano}-modified SPCEs also show a slight shift of the peak potentials of reduction/oxidation (E_{pc}/E_{pa}) with the increasing loading of Fe_{nano}, e.g., from −0.113/0.133 V (Fig. 2, curve a) at bare SPCEs to −0.186/0.176 V (Fig. 2, curve e) at Fe_{nano}-modified SPCEs with 0.4% Fe_{nano} loading. It implies that the effect of state density of $Fe(CN)_6^{4-/3-}$ redox couples on the heterogeneous electron transfer rate (k^o) at SPCE might have been changed.

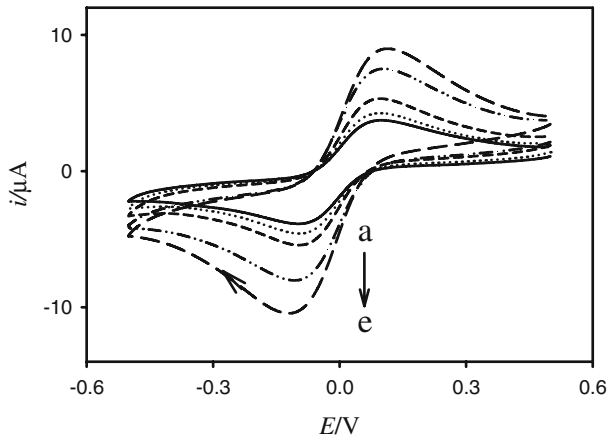

Fig. 2 Cyclic voltammograms of Fe_{nano}-modified SPCEs with different Fe_{nano} (w/v), **a** 0%; **b** 0.1%; **c** 0.2%; **d** 0.3%, and **e** 0.4% loadings in the presence of 0.1 M $Fe(CN)_6^{3-}$ solution. Scan rate was 0.05 V s^{-1}

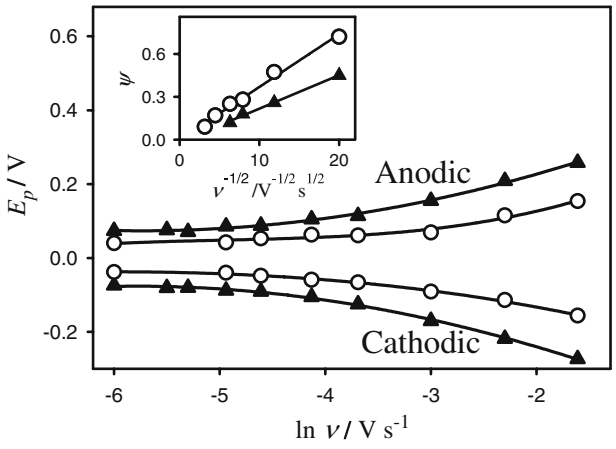

Fig. 3 Plots of the peak potential of (○) bare and (▲) Fe_{nano}-modified SPCEs by 0.4% (w/v) Fe_{nano} against the natural logarithm of the scan rate in the presence of 0.1 M $Fe(CN)_6^{3-}$ solution. *Inset*, plots of the corresponding parameter Ψ against inverse of square root of the scan rate

Therefore, Nicholson methodology [25] was adopted to clarify this effect as described in the following section.

Rate constant determination from CV with varying scan rate

Kinetic study was conducted at Fe_{nano}-modified and bare SPCEs with varying scan rate (υ). The increasing separation between the oxidation and reduction peaks potentials (ΔE_p) with increasing scan rate indicated the quasi-reversible process of the redox couples on electrodes (Fig. 3).

The Nicholson method is very useful to estimate the rate constant $k°$ for quasi-reversible reactions by determining ΔE_p vs υ, and then with the relation between ΔE_p and the parameter Ψ [25], which is defined as

$$\psi = \frac{(D_{Ox}/D_{Red})^{\alpha/2} k^{\circ}}{[D_{Ox}\pi\upsilon(nF/RT)]^{1/2}} \quad (1)$$

where D_{Ox} and D_{Red} are the diffusion coefficients of the oxidized and reduced forms, respectively, of the redox couple in solution, $Fe(CN)_6^{4-/3-}$ redox system exhibits a heterogeneous one-electron transfer (n=1), and the remaining terms have their usual electrochemical significance. Accordingly, the dependence of Ψ on $\upsilon^{1/2}$ should be linear (Fig. 3, inset), with the slope proportional to rate constant $k°$. Furthermore, some approximations should be made, by considering the diffusion coefficient D_{Ox}=D_{Red} with the known value of 8.0×10^{-6} cm^2 s^{-1} [24], at T=298°K, and Ψ became independent of the transfer coefficient α.

From Fig. 3 (inset) and Eq. (1), $k°$ values are calculated as 1.7×10^{-3} cm s^{-1} for bare SPCEs and 1.1×10^{-3} cm s^{-1} for Fe_{nano}-modified SPCEs, respectively. It is known that the rate of electron transfer at carbon-based electrodes depends on the structure and morphology of the carbon material used in the electrodes, and $k°$ value can be ranged from 10^{-4} cm s^{-1} to 10^{-2} cm s^{-1} for carbon-based electrodes with pretreatment or modification [26, 27]. In addition, it is found that $k°$ values for Fe_{nano}-modified and unmodified SPCEs are in the range of quasi-reversible reactions [28]. However, a lower value of $k°$ for Fe_{nano}-modified SPCEs is observed. It may be explained that the electroactive sites on the electrode surface are changed to be more hydrophobic toward redox couple solution after SPCEs being modified with Fe_{nano} [13].

Estimation of electroactive area

Electroactive area was used to characterize the carbon-based electrodes in many studies [16–18] by simple cyclic voltammetric analysis according to the Randles–Sevčik equation modified for quasi-reversible reaction [28]

$$i_p = K(\Lambda, \alpha) \times \left(2.69 \times 10^5\right) n^{3/2} A_{ea} C \sqrt{D}\sqrt{\upsilon} \quad (2)$$

where i_p is the peak current, A_{ea} is the electroactive area (cm^2), D is the diffusion coefficient (cm^2 s^{-1}), C is the concentration of the probe molecule in the bulk solution (mol cm^{-3}), $K(\Lambda, \alpha)$ is a modified parameter for quasi-reversible reaction with function of Λ, defined as $k°/[D(nF/RT)\upsilon]^{1/2}$,, and the transfer coefficient (α). The other terms have their usual significance.

Cyclic voltammetry was performed again over the potential range from +0.5 V to −0.5 V with scan rate of 0.05 V s^{-1} at both bare SPCEs and Fe_{nano}-modified SPCEs toward different $Fe(CN)_6^{3-}$ concentrations. The resulting cathodic peak currents (i_{pc}) were inhibited with increasing redox concentration as shown in Fig. 4. The modified parameter $K(\Lambda, \alpha)$ in Eq. (2) can be determined from ΔE_p and $E_{pc/2}$–E_{pc} [28], where E_{pc} and $E_{pc/2}$ are cathodic peak and half-

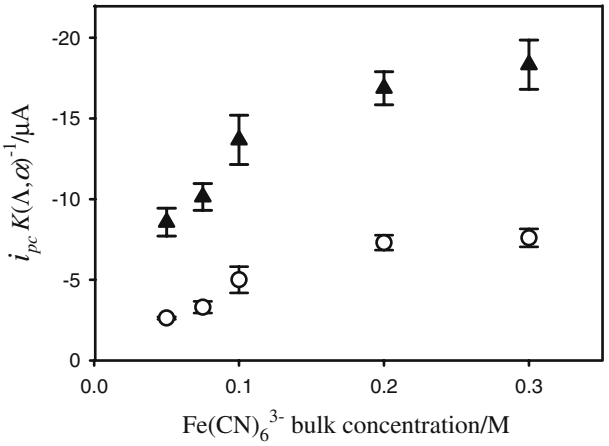

Fig. 4 Plots of $i_pK(\Lambda, \alpha)^{-1}$ obtained from cyclic voltammograms for (○) bare and (▲) Fe_{nano}-modified SPCEs by 0.4% (w/v) Fe_{nano} with varying concentration of $Fe(CN)_6^{3-}$; scan rate=0.05 V s^{-1}

peak potential, respectively. With substituting each calculated $K(\Lambda, \alpha)$ in the modified Randles–Sevčik Eq. (2) as follows,

$$i_pK(\Lambda,\alpha)^{-1} = 2.69 \times 10^5 n^{3/2} A_{ea} C\sqrt{D}\sqrt{\upsilon} \quad (3)$$

where the nonlinear response characteristics of the left term in Eq. (3) to the $Fe(CN)_6^{3-}$ concentration was illustrated in Fig. 4, and this effect complicated the estimation of electroactive area. It is noted that the SPCEs used in this study is difficult to produce notable i_p in the low $Fe(CN)_6^{3-}$ concentration ranges (<0.025 M). To reduce this effect, it was estimated from the slope of the linear region of the $i_pK(\Lambda, \alpha)^{-1}$ vs C plot at $C \rightarrow 0$ and A_{ea} yielded $7.1\pm0.9\times10^{-3}$ cm^2 for bare SPCEs, which is about 8.3% of its apparent geometric area (0.085 cm^2) without considering the roughness of the electrode. Meanwhile, an increased A_{ea} ($2.2\pm0.6\times10^{-2}$ cm^2) was obtained for the Fe_{nano}-modified SPCEs. The results are almost compatible to the SPCEs containing commercial carbon paste without any pretreatment in the report of Dock and Ruzgas [12].

Electrochemical recognition of Fe_{nano}-modified SPCEs by EIS

A common way of showing the resulting data is the Nyquist Plot, in which the real (Z') vs the imaginary (Z'') components of the impedance (Z) are plotted. When an AC current flows through a circuit made of resistors, capacitors, inductors, or any combination of these, the impedance, the ratio of applied voltage to measured current ($Z=E/I$),, shows a complex notation with the real part attributable to resistors and the imaginary part attributable to the capacitors $\left(Z = Z' + jZ; j = \sqrt{-1}\right)$. The interface can be modeled by a simplest equivalent circuit (Fig. 5), made of the electrolyte solution resistance (R_Ω) in series with the parallel circuit of Faradic impedance and double-layer

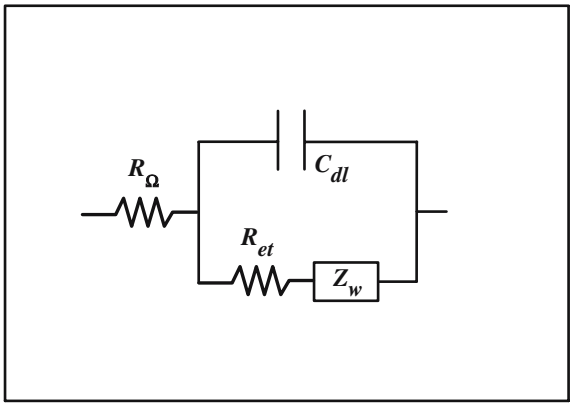

Fig. 5 A simple equivalent circuit for quasi-reversible electron transfer process

capacitance (C_{dl}). Here, Faradic impedance is composed of Warburg impedance (Z_w) and electron transfer resistance (R_{et}), whose expression can be derived from Butler–Volmer equation and, for small applied signal amplitudes, can be translated into the exchange current under equilibrium, i_0 [28].

$$R_{et} = RT(nFi_0)^{-1} \quad (4)$$

The exchange current i_0 [28] is given by the equation

$$\begin{aligned} i_0 &= nFA_{ea}k^\circ C_{Ox}\exp\left[-\alpha nF\left(E_{dc}-E^{\circ\prime}\right)/(RT)\right] \\ &= nFA_{ea}k^\circ C_{Red}\exp\left[(1-\alpha)nF\left(E_{dc}-E^{\circ\prime}\right)/(RT)\right] \end{aligned} \quad (5)$$

where C_{Ox} and C_{Red} are the bulk concentration of the oxidized and reduced form, respectively, of redox couple in solution, E_{dc} is the equilibrium dc-potential of the electrode, $E^{\circ\prime}$ is the formal potential of the redox couple in the solution, and the remaining terms have their usual significance. Under the experimental conditions used in this work, i.e., $E_{dc}=E^{\circ\prime}$ and $C_{Ox}=C_{Red}=C$, Eq. (5) reduces to

$$i_0 = nFA_{ea}k^\circ C \quad (6)$$

Combination of Eqs. (4) and (6) gives

$$A_{ea} = RT/\left(n^2F^2R_{et}k^\circ C\right) \quad (7)$$

where the electroactive area, A_{ea}, can be obtained. In this study, it was carried out with varying the total concentration of the $Fe(CN)_6^{4-/3-}$ redox couple but keeping $C_{Ox}=C_{Red}$ at the open-circuit potentials. A constant phase element (CPE) is often introduced in the equivalent circuit instead of a capacitance for a better fitting to stem from the fact that the electrode is normally rough and the deviation of real situation from the ideal behavior.

The Nyquist Plots with different dilute $Fe(CN)_6^{4-/3-}$ solutions for bare and Fe_{nano}-modified SPCEs are shown in Fig. 6, and R_{et} can be acquired by modeling of the

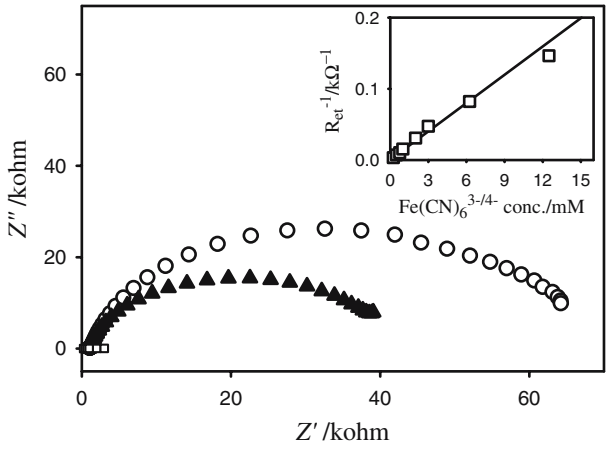

Fig. 6 Nyquist Plot at SPCEs in 1 mM $Fe(CN)_6^{4-/3-}$ concentration for (○) bare and (▲) Fe_{nano}-modified SPCEs by 0.4% (w/v) Fe_{nano}. *Inset*, plot of the reciprocal of R_{et} at bare SPCEs with good linear correlations (r^2=0.9993) against $Fe(CN)_6^{3-/4-}$ bulk concentrations (0.25, 0.5, 0.75, 1.0, 2.0, 3.0, and 6.0 mM)

impedance data using this simple equivalent circuit. It is indicated that the reciprocal of R_{et} depended linearly on $Fe(CN)_6^{4-/3-}$ concentration with very good regression (r^2=0.9993) up to 6.0 mM (Fig. 6, inset). From Eq. (7), the A_{ea} gives value 8.3±0.7×10^{-3} cm^2 for bare SPCEs and 2.4±0.3×10^{-2} cm^2 for Fe_{nano}-modified SPCEs, which are close to those obtained from CV, and this provides a validating evaluation of A_{ea}. Therefore, the amplified current at SPCEs with modification by Fe_{nano} is characterized with a

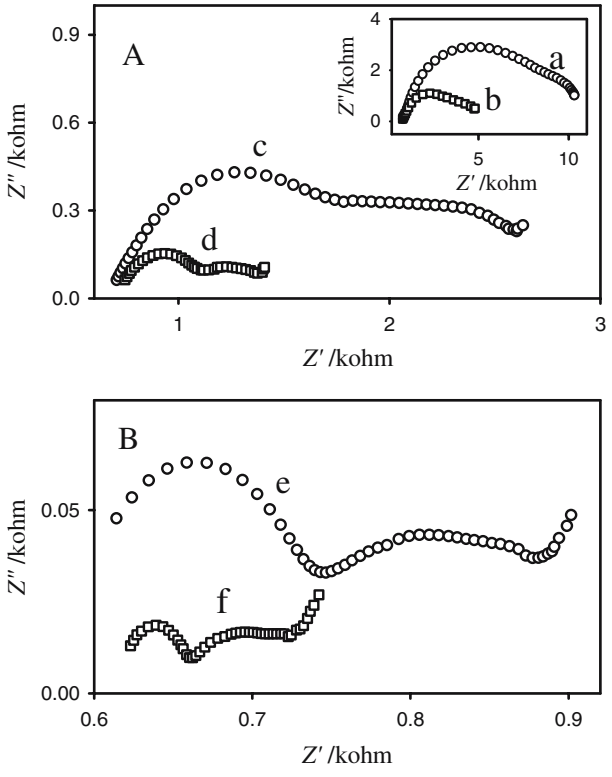

Fig. 7 Nyquist Plot at bare SPCEs in **a** 6.0; **b** 12; **c** 25; **d** 50; **e** 100; **f** 200 mM $Fe(CN)_6^{4-/3-}$ concentration

significant increase of A_{ea} due to the high electric properties of iron nanoparticles.

Depending on the types of electrochemical reactions involved at the interface, the equivalent circuit can be more complicated. The inhibited mechanism in Fig. 4 was further investigated by EIS. It was shown in Fig. 7A and B that a second semicircle at the moderate region of frequency appeared gradually with an increase in $Fe(CN)_6^{4-/3-}$ concentration at bare SPCEs. Similar curves can be obtained for Fe_{nano}-modified SPCEs (data not shown). Nyquist Plots together with the equivalent circuit that best fits these results are depicted in Fig. 8. It has been known that impedance behavior by Nyquist Plots with more than one semicircle may describe electrochemical systems with more complicated Faradaic processes (i.e., coating formation/deterioration or adsorption phenomena on the transducer as well as coupled chemical reactions). Indeed, EIS has also proved to be an effective method to probe the interface properties of surface-modified transducers [29].

In this study, the additional bulk resistance (R_b), derived from the second semicircle in parallel with a pure geometric capacitance (C_g), appeared as $Fe(CN)_6^{4-/3-}$ concentration is higher than 25 mM. It may be suggested that there is a barrier, which is resulted from blocking of decomposition products of active complex on the electrode surface [23, 24], for electron transfer between the electrode and the redox probe in solution. Similar result was also observed

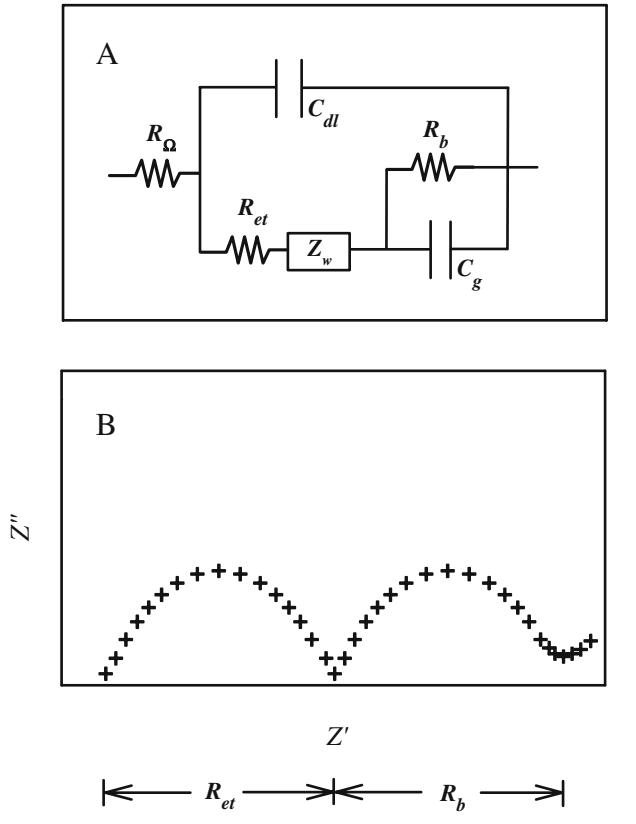

Fig. 8 Equivalent circuit (**a**) that best describe the impedance behavior of electrodes with deposition of decomposition products by active complex and their corresponding Nyquist Plot (**b**)

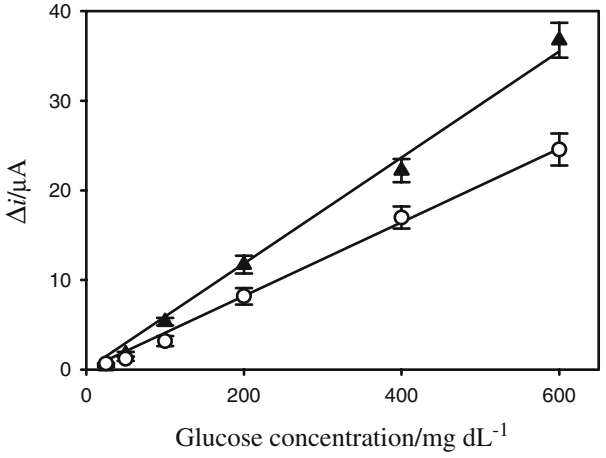

Fig. 9 Glucose calibration plots obtained from chronoamperometric recording at (○) $Fe(CN)_6^{3-}$/GOD-deposited and (▲) Fe_{nano}-$Fe(CN)_6^{3-}$/GOD-deposited SPCEs by 0.4% (w/v) Fe_{nano} at the operating potential of 0.3 V in supporting electrolyte of 0.1 M PBS (pH 7.0) (regression coefficient, r^2=(○) 0.9867 and (▲) 0.9731). Δi is the difference between the response currents in the presence and absence of glucose

by Winkler [24], who had investigated the dependence of electron transfer at platinum electrode on the $Fe(CN)_6^{4-/3-}$ redox concentration by using various voltammetric methods, and pointed that the electron transfer was inhibited by the partial blocking of electrode surface by $Fe(CN)_6^{4-/3-}$ decomposition products.

Calibration curve of glucose biosensing

Inasmuch as Fe_{nano}-modified SPCEs showed a higher electron transfer rate than unmodified SPCEs, further application for glucose biosensing was examined by using CA at fixed operating potential of 0.3 V. The difference between the response currents in the presence and absence of glucose (Δi) was obtained at 10 s, and the calibration curves were plotted with Δi against glucose concentration (Fig. 9). Results showed that both the $Fe(CN)_6^{3-}$/GOD and Fe_{nano}-$Fe(CN)_6^{3-}$/GOD-deposited SPCEs exhibited a linear response to glucose in the concentration range from 50 to 600 mg dl^{-1}. In addition, the Fe_{nano}-modified glucose-sensing strips demonstrated an increase of sensitivity from 0.043 to 0.062 μA mg^{-1} dl compared to the glucose-sensing strips without Fe_{nano} modification. According to the results from CV analysis (see "Estimation of electroactive area"), the enhanced sensitivity may be a major contribution to the increase of A_{ea} of SPCEs. Moreover, because the response sensitivity of the biosensor is proportional to the overall bio-electrochemical reaction rate as shown in Fig. 1, an increase of sensitivity may be expected as a result from the enhanced electron transfer rate. However, it was found that both the background and glucose-response currents increased simultaneously for Fe_{nano}-modified SPCEs. Therefore, a lower enhancement of the sensitivity for glucose detection compared to enhancement observed for redox current (in Fig. 2) was obtained.

Conclusions

The significant enhancement of electron transfer on SPCEs with modification by iron nanoparticles (Fe_{nano}), coupled with $Fe(CN)_6^{4-/3-}$ redox species, was characterized with an increase of electroactive area (A_{ea}) at electrode surface (2.4±0.3×10^{-2} cm^2) by a factor approximately 3 than the bare SPCEs (8.3±0.71×10^{-3} cm^2) and together with a decrease of the heterogeneous electron transfer rate constant. An inhibited diffusion current was observed from CVs with an increase in redox concentration for both SPCEs, and this effect complicated the estimation of electroactive area at electrode surface. It was attributed to the blocking of decomposition product of active complex that can be easily detected in the impedance spectra, similar to polymer-coated phenomena, by the appearance of a second semicircle in Nyquist Plot. Therefore, it provides a suitable method to evaluate the variety of carbon-based SPCEs with modification, taking into account the different properties of the carbon-paste compounds. In addition, a glucose biosensor with an increase of sensitivity from 0.043 to 0.062 μA mg^{-1} dl after the modification of SPCEs with 0.4% (w/v) Fe_{nano} is also presented.

Acknowledgements The authors thank Apex Biotechnology Corp. and the Ministry of Economic Affairs (Taiwan, ROC) for the financial support.

References

1. Turkusic E, Milicevic V, Tahmiscija H, Vehabovic M, Basic S, Amidzic V (2000) Fresenius J Anal Chem 368:466–470
2. Kumar AS, Zen J-M (2002) Electroanalysis 14:671–678
3. Choi J-Y, Seo K, Cho S-R, Oh J-R, Kahng S-H, Park J (2001) Anal Chim Acta 443:241–247
4. Neuhold CG, Wang J, do Nascimento VB, Kalcher K (1995) Talanta 42:1791–1798
5. Wang J, Zhang X (1999) Anal Lett 32:1739–1749
6. Lewis BD (1992) Clin Chem 38:2093–2095
7. Green MJ, Hilditch PI (1991) Anal Proc 28:374–377
8. Nagata R, Yokayama K, Clark SA, Karube I (1995) Biosens Bioelectron 10:261–267
9. Eftekhari A (2001) Sens Actuators B 80:283–289
10. Shulga AA, Koudelka-Hep M, de Rooij NF (1994) Anal Chem 66:205–210
11. Jaffari SA, Turner APF (1997) Biosens Bioelectron 12:1–9
12. Dock E, Ruzgas T (2003) Electroanalysis 15:492–498
13. Cui G, Yoo JH, Lee JS, Yoo J, Uhm JH, Cha GS, Nam H (2001) Analyst 126:1399–1403
14. Wang J, Tian B, Nascimento VB, Angnes L (1998) Electrochim Acta 43:3459–3465
15. Guo L, Huang Q, Li X, Yang S (2001) Phys Chem Chem Phys 3:1661–1665
16. Patel NG, Erlenkotter A, Cammann K, Chemnitius GC (2000) Sens Actuators B 67:134–141
17. Valentini F, Amine A, Orlanducci S, Terranova ML, Palleschi G (2003) Anal Chem 75:5413–5421

18. Hrapovic S, Liu Y, Male KB, Luong JHT (2004) Anal Chem 76:1083–1088
19. Zahl A, van Eldik R, Swaddle TW (2002) Inorg Chem 41:757–764
20. Bieman DJ, Fawcett WR (1972) J Electroanal Chem 34:27–39
21. Christensen PA, Hamnett A, Trevellick PR (1988) J Electroanal Chem 242:23–45
22. Kunimatsu K, Shigematsu Y, Uosaki K, Kita H (1989) J Electroanal Chem 262:195–209
23. Pons S, Datta M, McAleer JF, Hinman AS (1984) J Electroanal Chem 160:369–376
24. Winkler K (1995) J Electroanal Chem 388:151–159
25. Nicholson RS (1965) Anal Chem 37:1351–1355
26. Kneten KR, McCreery RL (1992) Anal Chem 64:2518–2524
27. Wang J, Kirgöz ÜA, Mo JW, Lu J, Kawde AN, Muck A (2001) Electrochem Commun 3:203–208
28. Bard AJ, Faulkner LR (2001) Electrochemical methods: fundamentals and applications, 2nd edn. Wiley, New York, pp 228–243 and 376–386
29. Amirudin A, Thierry D (1995) Prog Org Coat 26:1–28